

1984

Study of Space Charge Limitation of Thermionic Cathodes in Triode Guns

A. Delâge
National Research Council Canada

P. B. Sewell
National Research Council Canada

Follow this and additional works at: <https://digitalcommons.usu.edu/electron>

 Part of the [Biology Commons](#)

Recommended Citation

Delâge, A. and Sewell, P. B. (1984) "Study of Space Charge Limitation of Thermionic Cathodes in Triode Guns," *Scanning Electron Microscopy*: Vol. 3 : No. 1 , Article 17.

Available at: <https://digitalcommons.usu.edu/electron/vol3/iss1/17>

This Article is brought to you for free and open access by the Western Dairy Center at DigitalCommons@USU. It has been accepted for inclusion in Scanning Electron Microscopy by an authorized administrator of DigitalCommons@USU. For more information, please contact digitalcommons@usu.edu.



STUDY OF SPACE CHARGE LIMITATION OF THERMIONIC CATHODES IN TRIODE GUNS

A. Delâge and P.B. Sewell

Division of Electrical Engineering
National Research Council Canada
Ottawa, Ontario K1A 0R6
Canada

Abstract

A computer program has been developed to compute the emission of cathodes from the fully space charge limited diode equation. The emission of four different gun arrangements with thermionic cathodes of the type used in electron microscopes is investigated. Microflat cathodes with a small ($\leq 50\mu\text{m}$ in diameter) fixed emitting area show several advantages for high brightness possibilities whereas other types of cathodes for which the emitting area increases with the brightness are usually limited by too great a total emission.

Introduction

In electron microscopes equipped with thermionic sources, the filament is often used in the regime of space charge limitation in order to provide the gun with a higher stability. In this regime the electron emission is in principle determined entirely by the cloud of electrons produced in front of the cathode and is independent of the characteristic emission of the cathode itself, provided it can emit a sufficient number of electrons. The emission is then controlled by the field in front of the cathode and can be adjusted by varying the Wehnelt potential.

Since the life of the cathode is very dependent on its operating temperature, this is generally chosen such that the filament is on the border of the space charge limitation. This regime makes the emission independent of the filament temperature and the nature of the filament itself. The direct replacement of the tungsten filament by a better emitter such as LaB_6 would be almost imperceptible if the gun operating parameters remain the same.

In order to improve the brightness obtained from triode guns a detailed investigation of space-charge limitation is necessary.

Thermionic Emission

A computer program has been developed to calculate the emission from a cathode taking into account the space charge and the possible temperature limitation of the cathode. This program follows the technique described by Kirstein et al³. It is based on the theoretical maximum current that can be drawn from a one-dimensional diode. Before discussion of this technique, some basic concepts of thermionic emission are considered.

The simple model of the free electron gas in a metal⁷ describes successfully the thermionic emission of solids in terms of only two parameters: the temperature T and the work function ϕ associated with a particular metal. The model predicts a current density given by Richardson's equation:

KEY WORDS: Thermionic emission computation, Space-charge simulation, Thermionic cathodes, Microflat cathodes, Triode electron gun, Diode electron gun, Low voltage gun

Address for correspondence:
A. Delâge, Division of Electrical Engineering
National Research Council Canada, Ottawa, Ontario
Canada, K1A 0R6 Phone No.: (613) 993-2304.

List of Symbols

A	Constant in the Richardson's equation = 120 A.cm ⁻² .K ⁻²	V _{e1} (R,Z)	Solution of the potentials exclusively due to the electrode arrangement
D	Diameter (μm) of the emitting area in equation (14)	V _{sc} (R,Z)	Solution of the potentials exclusively due to the space charge in the gun
E	Electric field (V.m ⁻¹ if not specified)	V _{sc} ⁽ⁿ⁾	V _{sc} at the n th iteration
G	(4/9)ε ₀ (2e/m) ^{1/2} = 2.34 x 10 ⁻⁶ A.V ^{-1.5}	Z	Axial matrix coordinate (integer) in the network method
G'	G/z ₀	d	Separation cathode-anode in the diode model
I(r)	Current emitted by an annulus on the cathode, of mean radius r and a width Δr	dt	Integration step of the trajectory
I(r,n)	I(r) after the n th iteration	e	Electronic charge (1.602 x 10 ⁻¹⁹ C)
I _{tot} ⁽ⁿ⁾	Total current emitted after the n th iteration	h	Mesh size of the grid in the network method
J	Current density in A/cm ²	k	Boltzmann's constant 1.38 x 10 ⁻²³ J.K ⁻¹
J ₀	J given by Richardson's equation, also called the temperature limitation	m	Electronic mass 9.1 x 10 ⁻³¹ kg
J(T,E)	J given by Schottky's equation	n(v _z)dv _z	Density of electrons having a speed between v _z and v _z + dv _z
J _{sc}	Space charge limited J, also called the space charge limitation	r	The radial coordinate
J _D (E,D)	J _{sc} for the diode gun with a limited emitting area	r _d	Radius of the small area in the center of the cathode
N	Number of trajectories issued from each annulus on the cathode	v _x , v _y , v _z	Electron speeds in the model of electron gas in metal
N ₀	Density of electrons in the model of the electron gas in metal	z	The axial coordinate
Q(R,Z)	The space charge density term for each mesh of the grid used in the network method	z _m	Position of the potential minimum
R	Radial matrix coordinate (integer) in the network method	z ₀	Axial position where the Child-Langmuir equation is applied
S	Surface on the emitting cathode	β	Brightness in A cm ⁻² sr ⁻¹
T	Absolute temperature (K)	γ	Under-relaxation factor (0 ≤ γ ≤ 1; ideal value 0.667)
V _m	Potential minimum (V)	Δr	width of an emitting annulus on the cathode
V _A	Anode potential corresponding to the energy of the electrons at the anode (V)	Δvol	Volume element associated with each cell of the mesh in the network method
V(z)	Axial potential in the gun (V)	ε ₀	Vacuum permittivity 8.85 X 10 ⁻¹² C/V.m
		ϕ	Work function of the cathode material (V)

$$J_0(T, \phi) = A T^2 \exp(-e\phi/kT) \quad (1)$$

This equation gives the thermal limitation of the cathode. In fact the presence of the electron cloud or the presence of a purely attractive field E (without the electron cloud) will influence the height of the barrier that the electrons have to cross at the surface of the solid. In the first case the space charge gives a supplementary barrier (V_m on Fig. 1b) that will be added to ϕ while in the second case the reduction of the height of the barrier will lead to Schottky emission⁸:

$$J(T, E) = J_0 \exp \{0,4403 \sqrt{E/T}\} \quad (2)$$

(J and J₀ in A/cm², E in V/m and T in degree K).

In the mode of space charge limitation the barrier V_m produces an emission density simply given by⁴:

$$J_{sc} = J_0(T, \phi) \exp(-eV_m/kT) \quad (3)$$

As mentioned previously the local field in front of the cathode will determine the height of V_m. Unfortunately the relation between this field (prior to emission) and V_m is not known except for the case of a one-dimension diode.

In a general approach it is possible to compute the emission from this model. It consists of evaluating numerically the height of V_m by tracing the trajectories of the electrons considering a gaussian velocity distribution as

stated in the original gas model:

$$n(v_z)dv_z = N_0 \exp \left\{ -\left(v_x^2 + v_y^2 + v_z^2 \right) m / 2kT \right\} \quad (4)$$

This approach is very tedious since the number of trajectories to be calculated is very large and only an insignificant portion succeed in going through the barrier to form the beam⁹. It also contains another difficulty since it assumes that we have to resolve the distance z_m between the barrier and the cathode, a distance very small compared to the length of the beam.

However this procedure can be overcome by using a slightly different approach that includes the evaluation of the emission for the case of the one-dimension diode. The potential on the axis of such a cathode is presented in Fig. 1a with some enlargement on Fig. 1b for the region near the cathode. The curve A represents the potential prior to emission or for a highly temperature limited diode where the beam is so small that it does not affect the potential. The curve B represents the diode fully space charge limited. It is possible to find an analytical solution for this problem if we neglect the size of V_m and z_m by solving the Poisson equation in one dimension. This leads to a current density given by:

$$J [A/cm^2] = G V_A^{1.5} / d [cm]^2 \quad (5)$$

with $G = (4 \epsilon_0 / 9) \sqrt{2e/m} = 2.34 \times 10^{-6} A/V^{1.5}$.

Since the potential on the axis is given by $V(z) = V_A (z/d)^{4/3}$ an interesting conclusion from this approach is the following relation for the current density:

$$J = G V(z)^{1.5} / z^2 = G V_A^{1.5} / d^2 \quad (6)$$

This means that the current density can be evaluated at any location where the gun is fully space charge limited.

Another supposition is implicit in equation (6); the initial velocity of the electrons is zero so that both V_m and z_m are neglected. Some refinement of this solution consists of using the Child-Langmuir expression that takes into account the axial velocities in the beam. In the present case since the computations are done on a micro-computer and are not aimed at very large accuracy, this refinement is neglected.

However the conclusion for this diode may be generalised to the case of the triode gun (or any other gun geometry). For the triode gun the presence of the negatively charged Wehnelt modifies the axis potential in a way very similar to the space charge in the diode except for its external control. This control modifies continuously the potential in the gun from curve A to B in Fig. 1a without changing the temperature of the filament.

On the other hand two main differences exist. (1) The electron beam is now concentrated near the axis instead of filling all the space and consequently only the potential near the axis

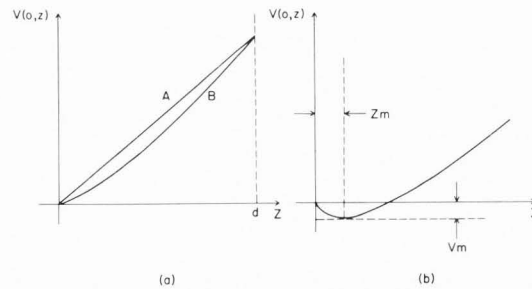


Fig. 1a Axial potential distribution in a diode (A) prior to emission and (B) at the full space-charge limitation.

Fig. 1b Enlargement of curve B in the vicinity of the origin.

will be affected by the beam. (2) The effect of the charge distribution on the Wehnelt has a much longer range than the space charge of the beam so that in practice only the region near the cathode where the slow electrons produce a large space charge will be affected by the space charge itself.

It is concluded from these remarks that to be valid the Langmuir equation (6) must be applied at a distance z_0 near the cathode much larger than z_m .

Numerical Evaluation of Cathode Emission

The technique used here to compute the emission of the gun has been adapted from the procedure described by Kirstein et al³. It consists of the following iterative procedure:

1. Solution of Laplace Equation; this solution is called here $V_{e1}(R,Z)$.
2. Division of the cathode in small areas according to the symmetry; in this case a disk and concentric annuli of width Δr ; a number (N) of trajectories issuing from the areas at different angles and/or energies.
3. Computation of $I(r)$ the total current associated to each beamlet or $I(r)/N$ for each trajectory.

$$I(r) = 2 \pi r \Delta r G V(r, z_0)^{1.5} / z_0^2.$$

4. Computation of the space charge from the trajectories. At each step of integration in the trajectories the following matrix element is computed:
 $Q(R,Z) = Q(R,Z) + I(r) dt h^2 / (\epsilon_0 \Delta V_0)$, h being the mesh size and ΔV_0 the volume element associated to each mesh.
5. Solution of Poisson Equation with 0 volt on the electrodes such that $V(R,Z) = V_{e1}(R,Z) + V_{sc}(R,Z)$.
6. Repeat from 3 until $I(r)$ converges.

Technically it appears that some time can be saved by introducing near the cathode a smaller boundary than the entire gun. The space charge is then computed numerically only in this region. The boundary itself is affected by the space charge but only in a small amount especially if it has been chosen properly.

Usually this boundary "converges" much more rapidly than $I(r)$ and very often only one iteration is necessary.

In the present approach it has been found very efficient to compute this boundary from the charge density method and to apply the finite difference method inside as suggested by Birtles¹.

The choice of z_0 may be somewhat controversial but since the mesh size (h) used inside the boundary is large, $z_0 = h$ seems adequate.

It has been proposed³ to increase the convergence of this problem by under-relaxing the choice of $I(r)$ so that the n th iteration is as follows:

$$I(r, n) = I(r, n-1)(1-\gamma) + \gamma I(r) \quad (7)$$

$$\text{with } 0 < \gamma \leq 1.$$

This technique can be improved by assuming that the space charge is directly proportional to the total current I_{tot} in the beam. This current is given by the following integral:

$$I_{tot}^{(n+1)} = G \int_S (V_{el} + v_{sc}^{(n)})^{1.5} dS. \quad (8)$$

Ideally when the value of the current converges, the solutions of the n th and $(n+1)$ th iterations are equal for large n so that we can write:

$$I_{tot}^{(n+1)} = G \int_S (V_{el} + v_{sc}^{(n+1)})^{1.5} dS. \quad (9)$$

If now we use this expression as very good approximation for $v_{sc}^{(n+1)}$:

$$v_{sc}^{(n+1)} = I_{tot}^{(n+1)} v_{sc}^{(n)} / I_{tot}^{(n)} \quad (10)$$

a much more accurate total beam current for the next iteration is given by solving equation (9). This later relation includes I_{tot} on both sides of the equation but it pays to solve it numerically since the time required for one full iteration cycle represents five to ten minutes on a small computer (HP 9836) compared to a few seconds ($\leq 5s$) to solve equation (9).

Once $I_{tot}^{(n+1)}$ is found, the much more accurate $v_{sc}^{(n+1)}$ as defined by equation (10) is used instead of $v_{sc}^{(n)}$ to compute $I(r)$. In this procedure the convergence applies only to the shape of the beam and the distribution of electrons in it, never to the total current. This improves the convergence because the value of current has a tendency to be highly oscillatory. Results show that 10% of the final value is reached at the first iteration and usually less than 1% at the second one.

Results and Discussion

This technique has been applied to the four different guns described in Table 1. The first

is highly space-charge limited due to its flat cathode and large Wehnelt-anode distance of 9mm. The emission of this gun is presented in Figure 2 as a curve of brightness vs total current; the theoretical model is compared to experimental measurements obtained in our laboratory. The theoretical brightness is obtained by applying Langmuir's equation⁵ for $V_A \gg kT$:

$$\beta \text{ (A/cm}^2\text{sr)} = I(0)eV_A / \pi^2 r_d^2 k T \quad (11)$$

where $I(0)/\pi r_d^2$ is the current density of the central beamlet leaving the cathode on the axis from a small circular area of radius r_d . The agreement between the model and the experimental results is remarkably good. The prime interest of this gun was to study the effect of reducing the field on the performance of the overall source. The results show a large space-charge limitation in the brightnesses and also some deterioration in the size of the cross-over as the distance anode-Wehnelt is increased, due to large interaction between electrons.

The second gun with a conical cathode on a shorter Wehnelt-anode separation is typical of a triode gun used in electron microscopes. The current density in the apex region and the total current as a function of the logarithm of the excess of the Wehnelt voltage (V_w) over the cut-off voltage (V_{co}) are presented in Fig. 3. The emitting area of the cone is also presented. The current density can be converted into brightness using the following equivalent to equation (11):

$$\beta \text{ (A/cm}^2\text{sr)} = J \text{ (A/cm}^2) e V / \pi k T \quad (12)$$

For the example presented here the current density is converted into brightness by multiplying $J \text{ (A/cm}^2)$ by $\sim 3 \times 10^4 \text{ sr}^{-1}$.

This graph shows how the emitting area increases with the field which is directly proportional to $V_w - V_{co}$. This increase is responsible for the difference in slope between the current density and the total current curves. From Figure 3 it is seen that a cathode operating at 10 A/cm^2 would emit about $150 \mu\text{A}$. However at higher cathode loadings such as 30 or 50 A/cm^2 , the total current would be 0.9 and 2 mA respectively. Such currents are beyond the range of commercial electron microscope power supplies.

This engineering limitation associated with large power dissipation is not the only argument against the conical cathode. Since the current reaching the sample is many orders of magnitude less than the emitted current, only the electrons emitted near the axis contribute finally to the signal while all others interfere with the quality of the beam optics.

In the first place, there is an energy dispersion caused in the gun by the interaction between electrons originating from the cone and the axial electrons⁵ and must be minimized when chromatic aberration of the lenses is the limiting factor encountered in the column.

Space-charge Limitations in Triode Gun

TABLE 1
Gun Geometries

Gun	I	II	III	IV
Cathode Type	Flat Disk	Cone on Cylinder	Microflat on Cone	Flat Diode
Cathode Size ^a (μm)	ϕ : 500 t: 750	Cone Angle: 90° Base ϕ : 400	Cone Angle: 90° $\mu\text{Flat } \phi$: 90 Emitting ϕ : 60	Emitting Circle of Diameter D
Cathode Height (μm)	250	200	100	-
Wehnelt Diameter (mm)	1	1	1	-
Wehnelt-Anode (mm)	9	4 in Fig.3 10 in Fig.4	10	4 ^b
High-Voltage (kV)	15	15	15	Variable

a) t = thickness

b) Distance cathode-anode

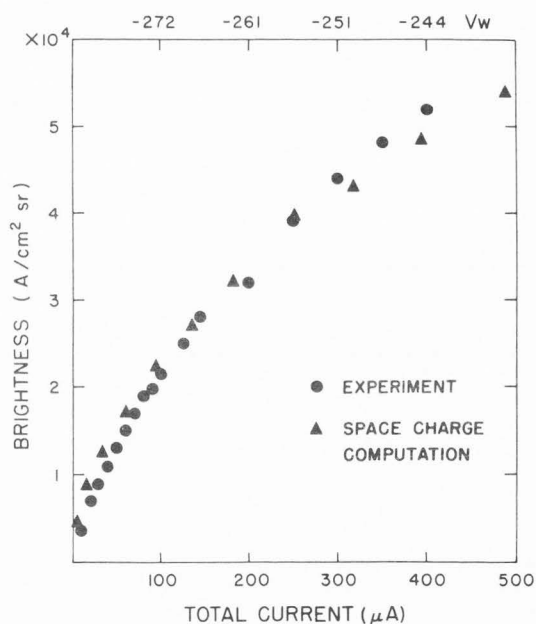


Fig. 2 Brightness vs total current characteristic for a flat cathode (gun I in Table 1).

Secondly the elimination of the undesirable electrons is not always hundred percent effective and stray electrons may contribute to the deterioration of the ideal performance of lenses and the sharpness of the central beam.

Finally an emitter tip with a finite radius of curvature can be represented by a portion of a sphere on the top of a truncated cone. This geometry contains two different electron optical systems with their own characteristics. At high

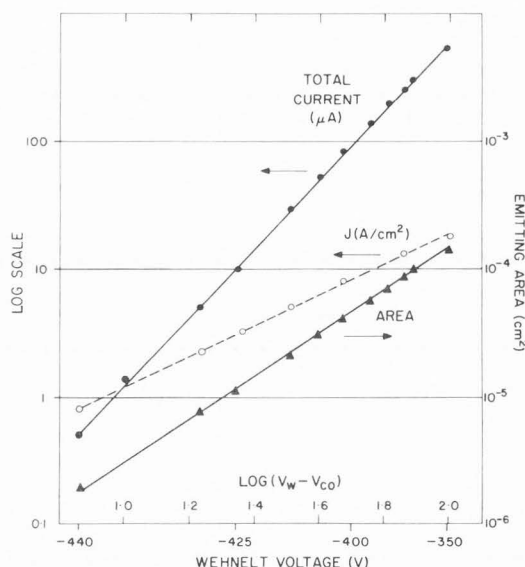


Fig. 3 Emission of a conical cathode (gun II in Table 1) as a function of the drive voltage ($V_W - V_{CO}$). The left hand log scale gives the values for the total current in μA and the current density at the apex in A/cm^2 .

negative bias, electron emission is confined to the tip region which results in good gun performance with high brightness¹⁰ and near-gaussian beam profile. At lower negative bias, emission from the walls of the conical surface leads to a complex beam form. For sintered LaB_6 cathodes this results in an additional complex ring structure around the central beam and for single-crystal LaB_6 an additional lobe pattern with crystallographic symmetry². In such a case

only a small portion of the beam is due to the desired paraxial electron emission. For the example discussed in Figure 3, if a conical cathode emitting at 10 A/cm^2 had a tip radius of curvature of $5 \mu\text{m}$, only 3% of the total current would come from the surface of the spherical tip.

The coated microflat cathode¹¹ has been designed to solve this fundamental difficulty. Some preliminary results on the emission of such cathode is presented in Figure 4. This conical cathode is coated and ground in such a way that the flat is $90 \mu\text{m}$ in diameter and exposes an LaB_6 area some $60 \mu\text{m}$ in diameter. The anode-Wehnelt distance is 10 mm and its performance can be directly compared to previous results obtained on flat cathodes (curve D) redrawn from Figure 2. The results for a pointed cathode in a 10 mm anode-Wehnelt spacing gun are also presented for comparison (curve C). The emission of the microflat is bounded in this figure by two curves: (1) the full space-charge limitation curve B and (2) the temperature limitation (curve A) given by the Richardson and Schottky equation:

$$\beta = J(T,E) / \pi k T \quad (13)$$

$$I_{\text{tot}} = J(T,E) \times \text{Microflat area}$$

The space charge limitation is computed from the model presented in this paper. If in this model we limit the cathode loading, the emission characteristic of this cathode goes from curve B to A following the paths shown in Figure 4. The numerical values on these paths correspond to the cathode loading in A/cm^2 . The curve C for the pointed cathode indicates much better performance near the cut-off but the effect of space-charge limits the current density to about 6 A/cm^2 at $400 \mu\text{A}$ of total emission while the fully space-charge limited microflat (curve B) is much less limited.

For the microflat cathode, this limitation is to a first approximation proportional to the total current and will be highly dependent on the area of emission. The fourth gun of Table 1 has been studied to investigate the influence of this area on the space-charge limitation. Microflat cathodes with small emitting areas can be used at zero bias potential ($V_W = 0 \text{ V}$) and give good performance, the current density being improved by Schottky emission¹¹. This suggests that this kind of cathode can be used in a diode gun. Considering that the diode gun is a limiting case for the triode gun as far as the field is concerned, some conclusions on the maximum brightness of a triode gun can be computed from this study.

The model of the diode gun consists simply of two planes, one of which forms the anode at potential V and a second one, the cathode, is allowed to emit only from a small circular region. The emission properties are studied as a function of the potential V and the diameter (D) of the emitting area. If the distance anode-cathode (here 4 mm) is much larger than D , the

current density emitted depends mainly on the mean field E in the diode and the size of the emitting area. For computation of E in the range $0.01 \leq E \leq 0.5 \text{ kV/mm}$ and $20 \leq D \leq 80 \mu\text{m}$ the axial current density is very well represented by the empirical formula:

$$J_D (\text{A/cm}^2) \cong 260 E(\text{kV/mm})^{1.5} / D(\mu\text{m})^{0.5} \quad (14)$$

where practical units have been used and are given in parenthesis.

Figure 5 gives a representation of the space charge limitation in terms of brightness reduction as a function of the voltage (representing the beam energy). The space-charge limitation effects occur only at low voltage. The two sets of curves give the percentage brightness loss for two different cathode temperatures 1800 and 1900 K for which $J(T,E=0)$ is respectively 10 and 30 A/cm^2 . Each set of curves has been computed for $D = 5, 10, 25, 50$ and $100 \mu\text{m}$ assuming that relation (14) can be extrapolated when necessary. Those results are computed from the following relation:

$$\beta \text{ Loss (\%)} = 100\% (1 - J_D / J(T,E)) \quad (15)$$

where J_D is given by equation (14) and $J(T,E)$ by equation (2).

For the lower temperature case ($J = 10 \text{ A/cm}^2$), the gun starts to be space charge limited for beam energies around 2.2 keV when the emitting area is $100 \mu\text{m}$. This pin-points the difficulty of using the standard triode gun for scanning electron microscopy application at low voltages. If a $10 \mu\text{m}$ microflat can be made, one can expect to use this kind of cathode without space charge limitation at 1 keV . Such low voltage operation is desirable for inspection of microelectronic devices without causing serious damage⁶.

Severe limitations are placed on the size of the microflat if full advantage is to be made of the emission of LaB_6 at low voltages. The set of curves at higher temperature gives a threshold of 2 keV for a $10 \mu\text{m}$ diameter microflat before space-charge limitation occurs.

Conclusion

The agreement between experimental and theoretical results presented in this paper indicates that the procedure described by Kirstein et al.³ does apply very well to triode guns. This technique has been used to study the space-charge effects of different types of cathodes, namely conical and microflat cathodes. The conical uncoated cathodes give very good performance near the cut-off where only the very tip is involved in the emission. On the other hand the emission from the cone usually gives too much current before the field at the apex increases enough to reach the full theoretical axial brightness. The coated microflat cathode which suppresses emission from the cone is much less prone to space-charge limitation and is more suitable for application where high brightness is required, especially at low voltages.

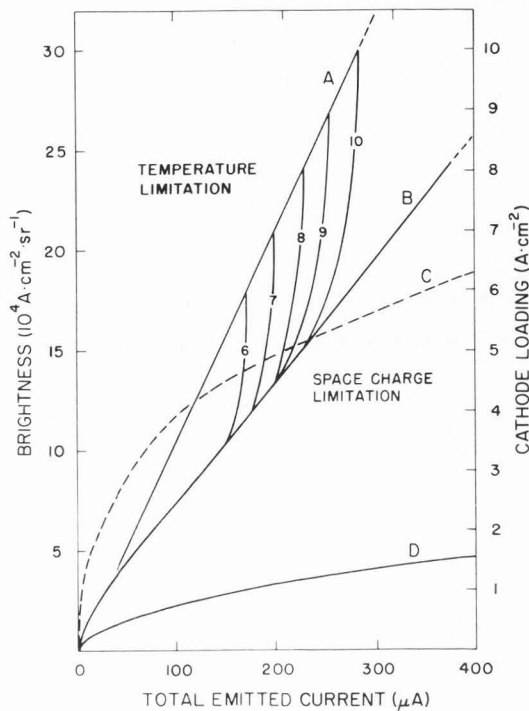


Fig. 4 Brightness vs total current characteristic for a microflat cathode (gun III in Table 1) for different cathode loadings (index in A/cm^2). Curves A and B are respectively the temperature and the space-charge limitation curves. The microflat is compared to a flat cathode (curve D) and a pointed cathode in a similar gun (curve C).

References

1. Birtles A.B., (1972) "An efficient technique for electrostatic field computation in some axially symmetric electron optics system", *Int. J. Electronics* **33**, 649-657.
2. Furukawa Y., Yamabe M. and Inagaki T., (1983) "Emission characteristics of single-crystal LaB_6 cathodes with large tip radius", *J. Vac. Sci. Technol.* **A1**, pp 1518-1521.
3. Kirstein P.T., Kino G.S., Waters W.E., (1967) *Space-Charge Flow*. McGraw Hill, New York, Chapter VIII, pp377-399.
4. Kirstein P.T., Kino G.S., Waters W.E., (1967), *ibid.*, Chapter VI, pp263-276.
5. Lauer R., (1982) "Characteristics of triode electron guns", in *Advances in optical and electron microscopy*, Vol. 8, Barer R. and Cosslett V.E. Eds., Academic Press, London, pp137-202.
6. Lukianoff G.V. and Langner G.O., (1983) "Electron beam induced voltage and injected charge modes of testing", *Scanning* **5**, pp 53-70.

LaB_6 MICRO FLAT

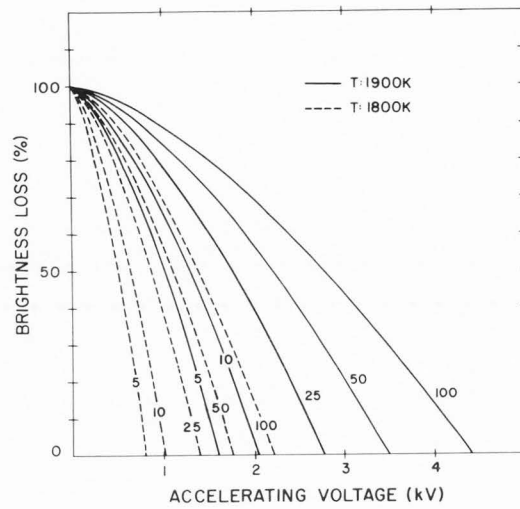


Fig. 5 Brightness loss at low energy for a microflat cathode in a diode gun (gun IV in Table 1) for two temperatures; curve indices are the microflat diameters in μm .

7. Nottingham W.B., (1956) *Thermionic Emission*, in *Handbook der Physik*, Volume XXI, Springer-Verlag Berlin. Section 17-18, pp14-17.
8. Nottingham W.B., ((1956), *ibid.*, Section 27, 28-33.
9. Renau A., Read F.H. and Brunt J.N.H., (1982) "The charge-density method of solving electrostatic problems with and without the inclusion of space-charge", *J. Phys. E: Sci. Instrum.* **15**, pp347-354.
10. Sewell P.B., (1980) "High brightness thermionic electron guns for electron microscopes", *Scanning Electron Microsc.* 1980; **I**: pp11-24.
11. Sewell P.B. and Delège A., (1984) "Thermionic emission studies of Micro-flat single crystal LaB_6 cathodes", in: *Electron Optical Systems*, 3rd Pfefferkorn Conf. Proceedings, SEM, Inc., AMF O'Hare, IL 163-170.

Discussion with Reviewers

J. Orloff: The coating of carbon on the microflat cathode will have an evaporation rate which is much less than that of the LaB_6 . The rate of evaporation or thickness loss, of LaB_6 is about 0.01 micrometers per hour at 1800 K and about 0.1 micrometers per hour at 1900 K. This means that the electron-emitting surface of the cathode will retreat behind a shell of carbon at some rate, depending on the cathode temperature. Can you comment on the effect this will have on the performance of the cathode?

Authors: Essentially the recess of LaB_6 with time will cause a non-uniform decrease in the field in front of the cathode, the drop being more

important on the outermost part of the emitting area near the carbon shell.

When the cathode is used in a standard gun with a field larger than 1 or 2 kV/mm the resulting electrical field will not affect the axial brightness which is usually temperature limited for this type of cathode.

On the other hand the effects of the recess will appear at low energy below the threshold where the emission is space-charge limited. These effects are (1) a drop in the emission current, (2) a decrease in the axial brightness and finally (3) an increase in the convergence of the beam due to the non-uniformity in the change in the field.

The total emission will be reduced significantly in those conditions because the part of the cathode that emits the most of the current is the most affected; consequently, the brightness will not decrease as much since the space-charge due to the total current will be less; this effect will partially compensate for the drop in the field.

The following table gives some figures for those effects; the computations have been carried out on the gun IV for a field of 0.1 kV/mm on a microflat of 50 μm . Results show that after 1000 hours of operation (at a loss of .01 $\mu\text{m}/\text{h}$) the brightness will be 54% of its original value for a microflat 50 μm in diameter.

RECESS (μm)	TOTAL CURRENT (%)	BRIGHTNESS (%)
0.0	100	100
2.5	67	92
5.0	45	80
7.5	32	67
10.0	23	54
12.5	17	43